Physica B 406 (2011) 354–357

Contents lists available at ScienceDirect

Physica B

journal homepage: www.elsevier.com/locate/physb

Experimental and theoretical Compton profiles of Be, C and Al

Julio C. Aguiar [a,b,*], Hector O. Di Rocco [b], Andrés Arazi [c]

[a] Autoridad Regulatoria Nuclear, Av. Del Libertador 8250, C1429BNP, Buenos Aires, Argentina
[b] Instituto de Física "Arroyo Seco", Facultad de Ciencias Exactas, U.N.C.P.B.A., Pinto 399, 7000 Tandil, Argentina
[c] Laboratorio TANDAR, Comisión Nacional de Energía Atómica, Av. General Paz 1499, 1650 San Martín, Buenos Aires, Argentina

ARTICLE INFO

Article history:
Received 25 August 2010
Accepted 25 October 2010

Keywords:
Compton profile
Compton scattering
Fermi momentum
Hartree Fock, Slater-type orbital

ABSTRACT

The results of Compton profile measurements, Fermi momentum determinations, and theoretical values obtained from a linear combination of Slater-type orbital (STO) for core electrons in beryllium; carbon and aluminium are presented. In addition, a Thomas–Fermi model is used to estimate the contribution of valence electrons to the Compton profile. Measurements were performed using monoenergetic photons of 59.54 keV provided by a low-intensity Am-241 γ-ray source. Scattered photons were detected at 90° from the beam direction using a p-type coaxial high-purity germanium detector (HPGe). The experimental results are in good agreement with theoretical calculations.

1. Introduction

Compton scattering can be understood as an inelastic scattering of X or gamma rays on electrons in a material medium [1]. Only a part of the incident photon energy is transferred to the electron, which is ejected from its orbit due to the large momentum transfer, and the new photon is scattered off at a lower energy. This is commonly called incoherent scattering.

Experimental study of Compton profile consists of the spectral measurement of scattered photons through a sample under study. This method has been widely used as a tool to extract information about the electronic structure of atoms in solid, liquid and gas [2,3].

In these experiments, a broadening of the Compton line is observed in the spectrum due to motion of electrons within the atom, which is known as atomic Doppler effect. Typically, the spectral measurement is achieved with the use of a high spectral resolution device, e.g. high-purity germanium (HPGe) detector.

Historically, experiments for determining the Compton profile (CP) were mounted for the study of free atoms (gas) and the results were compared with the so-called impulse approximation [4–6]. Experimental results for free atoms of He, Ne, Ar, Kr and Xe are in good agreement with theoretical values of the extensive Hartree–Fock (HF) Compton profiles table published by Eisenberger and Platzmann [4], Eisenberger and Reed [5], Holm and Ribberfors [6] and Biggs et al. [7].

Other authors have computed the spherical average Compton profiles using self-consistent Hartree–Fock wave functions employed on linear combination of atomic orbital (HF-LCAO) approximation [8].

Experimental results for Compton profile with Fermi momentum determination of Be, Al (in metal form) and C (in graphite form) are presented in this work. These results are compared with theoretical calculations expressed in terms of single-electron basis set for internal orbital by using linear combinations of Slater-type orbital (STO). The Fermi momentum for each one of the elements under study has been estimated experimentally from the results reported in this work.

2. Theoretical procedures

The radial wave functions $P_{nl}(r)$ for bound electrons of Be($1s^2$); C($1s^2$) and Al($1s^2\,2\,s^2$ and $2p^6$) are obtained by using of a self-consistent HF program (RCN) developed by Cowan and modified for this work. The Cowan program can be obtained at http://www.tcd.ie [9,10].

The output of the modified Cowan program produces numerical files which be identified as $P_{nl}^{HF}(r)$, then a fit of the tabulated functions by linear combination of STO is made. STO is used due to very simple analytical form of $P_{nl}(r)$ in radial representation.

A normalized linear combination of Slater functions can be represented by a convenient sum of terms $F_{nl}(r)$, which are expressed by

$$F_{nl}(r) = \frac{(2\zeta)^{n+1/2} r^{n-1} e^{-\zeta_{nl} r}}{\sqrt{(2n)!}} = N(n,\zeta)\, r^{n-1} e^{-\zeta_{nl}\, r} \quad (1)$$

where N is a normalization term in atomic unit (a.u.), i.e. $=m=e=1$ and $c=137$. ζ_{nl} is the effective nuclear charge expressed as

* Corresponding author at: Autoridad Regulatoria Nuclear, Av. Del Libertador 8250, C1429BNP, Buenos Aires, Argentina. Tel.: +54 11 6323 1370; fax: +54 11 6323 1375.
E-mail address: jaguiar@arn.gob.ar (J.C. Aguiar).

0921-4526/$ - see front matter © 2010 Elsevier B.V. All rights reserved.
doi:10.1016/j.physb.2010.10.062

$\zeta_{nl}=(Z-\sigma_{nl})/n$, with σ_{nl} the screening parameter, n the principal quantum number and r is the distance of the electron from the atomic nucleus in units of α_0 (Bohr radius).

The effective nuclear charge of internal lobes are obtained from the respective HF moments $\langle r^{-1}\rangle$, because $\zeta_{nl}=n^2\langle r^{-1}\rangle$ for both types of orbital (hydrogenic and Slater). For the external lobes, one of the charges is taken from the HF values of $\langle r^{-1}\rangle$, whereas the other ζ_{nl} is just another parameter to adjust.

As an example, consider the Al-like 3s orbital case; $P_{3s}(r)/r=R_{3s}(r)$, this can be expressed as

$$R_{3S}(r)=a_{1S}F_{1S}(r)+a_{2S}F_{2S}(r)+a_{3S1}F_{3S1}(r)+a_{3S2}F_{3S2}(r) \quad (2)$$

where the coefficients a are adjusted by the Taylor–Newton–Gauss fitting procedures. All basis set equations in the STO form are considered to be "minimal" basis sets for each output of Cowan program to a file $R_{nl}^{HF}(r)$. This is adjusted point by point through functions like those given by Eq. (2): single-Z for internal lobes and double-Z for external ones. a are constants to be determinated by analytical interaction using HF wave functions and the last lobe effective charge, as well.

For the construction of $R_{nl}(r)$ each atomic orbital is expressed as the sum of two or more STOs. The internal contributions to the given (n,l) need one Slater function whereas the more external lobe needs two Slater functions. In this case, each STO represents a different size orbital because of the different effective nuclear charge. This rule is valid for internal and external orbital of free atoms.

Table 1 lists the different values of a, b, c, d and ζ_{nl} used in these calculations.

As is well known, the electronic configuration of free Beryllium atom is $1s^2$, $2s^2$, but only $1s^2$ is confined within the internal lobes, similar thing happens for Carbon ($1s^2$) and Aluminium ($1s^2, 2s^2, 2p^6$). These internal orbitals contributions to Compton profile are approximate through of the use Slater-type orbital.

It can be demonstrated that, for the normalized Slater radial functions of the type Eq. (1), the Fourier transform (that is, Hankel transform for the radial part) takes the form [11],

$$\chi_{nl}(p)=N(n,\zeta)\frac{2\sqrt{2}\,\Gamma(n+l+2)p^{l+1}}{2^{l+2}p\zeta^{n+l+2}\Gamma(l+3/2)}\left\{{}_2F_1\left(\frac{n+l+2}{2},\frac{n+l+3}{2};l+\frac{3}{2};\frac{-p^2}{\zeta^2}\right)\right\} \quad (3)$$

where ${}_2F_1$ is a hypergeometric function and P is the momentum of an electron in the atom.

$${}_2F_1(a,b;c;z)=\sum_{k=0}\frac{(a)_k(b)_kz^k}{(c)_kk!} \quad (4)$$

with

$$(a)_k=a(a+1)(a+2)\cdots(a+k+1) \quad (5)$$

The electron momentum density for electrons of momentum p can be determined as follows

$$I_{nl}(p)=p^2\left|\chi_{nlm}(p)\right|^2 \quad (6)$$

Thus, in an isotropic system the Compton profile is defined as

$$J_{nl}(q)=\frac{1}{2}\int_{|q|}^{\infty}\frac{I_{nl}(p)}{p}dp \quad (7)$$

being

$$q(E)=-137\frac{E_i-E_f+E_iE_f(1-\cos\theta)/m_0c^2}{(E_i^2+E_f^2-2E_iE_f\cos\theta)^{1/2}} \quad (8)$$

Table 1
Values of a, b, c, d and ζ_{nl} used in STO calculations for free atom.

P_1s	Be	C	Al
a	0.98974	0.99199	0.99288
ζ1s1	3.68300	5.67000	12.6400
b	0.02131	0.01744	0.01388
ζ1s2	1.04638	1.49727	3.68562
P_2s	Be	C	Al
a	0.20095	0.23631	0.29250
ζ1s1	3.68300	5.67000	12.6400
b	0.72167	−0.35049	−0.93482
ζ2s1	2.0924	3.60120	8.29228
c	−1.73674	−0.67792	−0.10434
ζ2s2	1.98741	3.05245	8.32523
P_2p		C	Al
a		0.31340	0.32502
ζ2p1		5.13215	13.5422
b		0.75611	0.73031
ζ2p2		2.37388	6.93879
P_3p			Al
a			0.17565
ζ2p1			8.8280
b			−0.45307
ζ3p1			4.20927
c			−0.61210
ζ3p2			2.47727
P_3s			Al
a			0.07514
ζ1s1			12.6400
b			−0.24925
ζ2s1			9.4360
c			0.68045
ζ3s1			4.5774
d			0.35609
ζ3s2			3.25136

In this expression $m_0c^2=511.0034$ keV, E_i and E_f are incident and scattered photon energy, respectively; $q(E)$ is an experimental parameter extracted from spectral measurements after the deconvolution with the instrumental resolution function and is defined as the change of the photon momentum [12].

Thus, taking into account only the shell electrons closed, the Compton profile can be estimated by separated sum of $J_{nl}(q)$, using Eq. (7).

Moreover, several authors have proposed to estimate the Compton profile of free-electrons gas using Thomas–Fermi theory [13–15].

The contribution of valence electrons to the Compton profile can be expressed by the following equation

$$J_{val}^{element}(q)=\begin{cases}\dfrac{3n_{val}(p_F^2-q^2)}{4p_F^3}, & \text{for} \quad q<p_F\\ 0, & \text{for} \quad q\geq p_F\end{cases} \quad (9)$$

where p_F is the Fermi momentum in atomic units, this is experimentally obtained from the curve shown in Fig. 3, and n_{val} is the number of free electrons per atom, 2, 4 and 3 respectively, for Be, C and Al.

Thus, the problem of determining the shape of the Compton profile is reduced to the sum of Eqs. (7) and (9), i.e., $J_{1s}(q)+J_{2s}(q)+\cdots+J_{val}^{element}(q)$. These theoretical results calculations for Be (metal), C (graphite) and Al (metal) are presented in Fig. 3.

3. Experimental procedures

The Compton profile of Be, C and Al of high purity (better than 99.98%) with different thickness (5, 6 and 1 mm) was measured using an annular source of ^{241}Am (59.54 keV) with an activity of 7×10^9 Bq, property of National Commission of Atomic Energy of Argentina.

Four 2-cm-thick lead plates with identical open holes ($\phi = 0.5$ cm) were used as collimators. All measurements were performed at 90° according to the experimental geometry outlined in Fig. 1.

A p-type high-purity germanium detector with a 60% relative efficiency and 231 cm^3 crystal volume was used to detect the Compton peak. The instrumental resolution function was obtained by using multiple calibration sources of ^{210}Pb, ^{241}Am, ^{57}Co and ^{137}Cs with corresponding peaks of 46.5, 59.5, 122, 136 and 661.6 keV, respectively. The detector output spectrum was preset to 8192 channels. The full width at half maximum (FWHM) was determined to be

$$\mathrm{FWHM} = 0.841 + 1.1 \times 10^{-3}E - 3.14 \times 10^{-7}E^2 \quad (10)$$

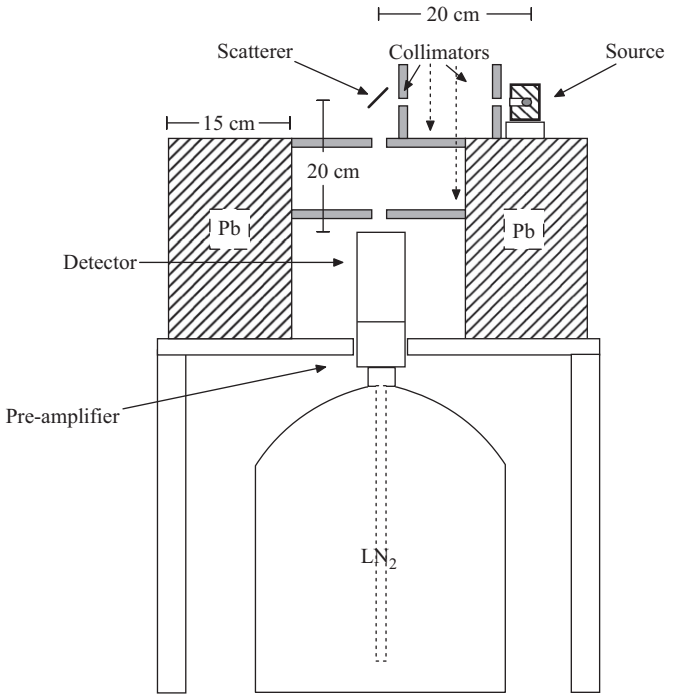

Fig. 1. Geometry and shielding of the experimental setup.

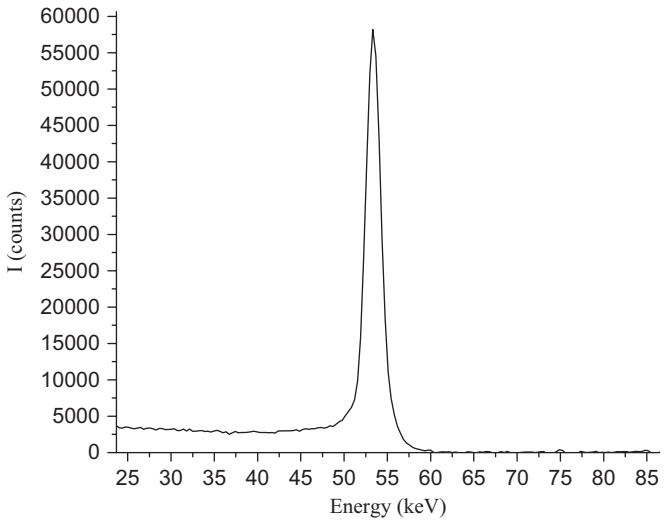

Fig. 2. Compton spectrum at 90° for graphite sample with background subtraction. The full-energy peak is observed to be 53.32 keV with FWHM = 2.092 keV.

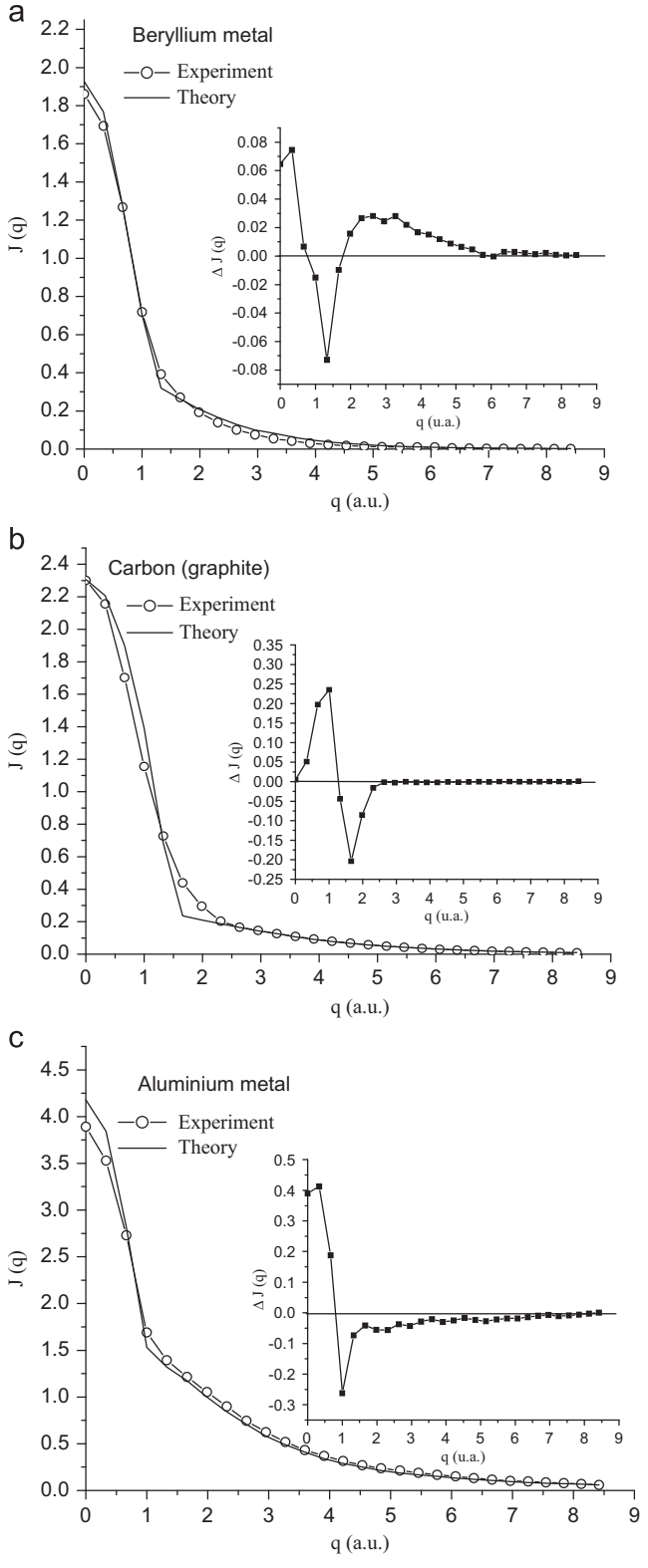

Fig. 3. Comparison of experimental and theoretical Compton profile results for (a) beryllium (metal), (b) carbon (in graphite form) and (c) aluminium (metal). The experimental errors are within the size of symbols used. Theoretical and experimental differences are presented in the insets.

The Digital Spectrum Analyzer (DSA-2000) was fully integrated; all of the subsystems required for high quality spectrum acquisition were integrated to the unit with high voltage power supply, digital stabilizer, MCA memory and Ethernet network interface (Canberra Inc., Meriden, CT, USA).

Experimental results of Compton profile were obtained after subtracting the background as shown in Fig. 2. Double scattering correction was applied; this procedure is described in previous works made by Williams [2] and Cooper et al. [3]. The Compton scattering spectrum was converted into momentum spectrum to find the $J(q)$ as a function of q and this was normalized to $2\int J(q)dq = Z$, where Z is the atomic number of the element under study (Fig. 3).

4. Results and discussion

The FWHM of the Compton peak at 53.32 keV is predicted, according to Eq. (10), to be 0.890 keV. However, the FWHM for beryllium metal, carbon graphite and aluminium metal were 1.988, 2.092 and 2.287 keV, respectively. This difference can be due to the broadening of the Compton line (Doppler effect).

The deconvolution in Compton profiles measurements was based on finding a theoretical Gaussian curve of the photo-peak for the same energy using the width at half maximum of 0.890 keV. This was made with help of ORIGIN-PRO 8 Lab-data analysis program (Origin Corporation, Northampton, MA 01060, USA).

The experimental results are in good agreement with theoretical calculations, except for some points of the curves (Fig. 3), where the discrepancy is however less than 20%. This difference can be due to the limitation of the Thomas–Fermi model that makes a sharp cut at top on the closed shells electrons.

However, comparing these results to $q=0$ with the ones from other authors a discrepancy less than 1, 2, 5% is observed for beryllium, carbon and aluminium, respectively [16–18].

Fig. 2 shows a Compton spectrum to 90° for graphite sample with background subtraction. The measurement time was 200,000 s; collecting 1.43 γ/s to 53.32 keV and with FWHM = 2.092 keV.

Values of Fermi momentum used in Eq. (9) were extracted from experimental curves. This can be seen as the contribution of valence electrons to the Compton profile with a cutoff at the Fermi momentum (see Fig. 3). In these curves it can be observed that Fermi momentum in atomic units are 1.06 (beryllium metal), 1.50 (carbon graphite) and 0.93 (aluminium metal).

5. Conclusions

In summary, the experimental results of beryllium metal, carbon graphite and aluminium metal are in good agreement with theoretical calculations by using Slater-type orbital and Thomas–Fermi model. In this way, an analytical approach for the Compton profile can be achieved for all the atomic systems including metal materials. This method can be proven to be valid at the moment at least for low-atomic number elements.

Acknowledgements

The authors wish to acknowledge the support from the Universidad Nacional del Centro (UNCPBA, Argentina) and the Consejo Nacional de Investigaciones Cientificas y Técnicas (CONICET, Argentina) and the help of the library staff of Nuclear Regulatory Authority of Argentina, especially Alicia Carregado, Mirta Hisano and Paula Garraza.

References

[1] A.H. Compton, Phys. Rev 22 (1923) 409.
[2] B.G. Williams (Ed.), McGraw-Hill, New York, 1977.
[3] M.J. Cooper, P.E. Mijnarends, N. Shiotani, N. Sakai, A. Bansil, X-ray Compton Scattering, Oxford University Press, New York, 2004.
[4] P. Eisenberger, P.M. Platzmann, Phys. Rev. A 2 (1970) 415.
[5] P. Eisenberger, W.A. Reed, Phys. Rev. A 5 (1972) 2085.
[6] P. Holm, R. Ribberfors, Phys. Rev. A 40 (1989) 6251.
[7] F. Biggs, L.B. Mendelsohn, J.B. Mann, Atom. Data Nucl. Data Tables 16 (1975) 201.
[8] R. Vijayakumar, N. Shivaramu, Ramamurthy, M.J. Ford, Physica B 403 (2008) 4309.
[9] R.D. Cowan, The Theory of Atomic Structure and Spectra, University of California Press, Berkeley, 1981.
[10] 〈http://www.tcd.ie/Physics/People/Cormac.McGuinness/Cowan/〉.
[11] P. Kaijser, V.H. Smith Jr., Adv. Quantum Chem. 10 (1977) 37.
[12] J.E. Fernandez, V. Scot, Nucl. Instrum. and Meth. B 263 (2007) 209.
[13] R. Weiss, X-ray Determination of Electron Distributions, North-Holland, 1966.
[14] N. Ashcroft, N. Mermin, Solid State Physics, Harcourt, Inc., 1976.
[15] G.P. Das, P. Chaddah, Solid. State Commun. 45 (1983) 607.
[16] G. Loupias, J. Petiau, A. Issolah, M. Schneider, Phys. Status Solidi B 102 (1980) 79.
[17] M.O. Hai-ding, G. Ying, G. Zhu-fang, Y. Bao-zhong, W. Tie-jun, B. Zu-he, Chin. Phys. Lett. 13 (1996) 5.
[18] G.S. Sohoni, D.G. Kanhere, Solid. State Commun. 48 (1983) 619.